Electronic Supplementary Material (ESI) for Physical Chemistry Chemical Physics.

Looking for chiral recognition in photoinduced bimolecular electron transfer using ultrafast spectroscopy

Pragya Verma, Christoph Nançoz, Johann Bosson, Géraldine M. Labrador, Jérôme Lacour, and Eric Vauthey*

Department of Physical Chemistry, University of Geneva, 30 Quai Ernest-Ansermet, 1211 Genève 4, Switzerland

Contents

S1 Samples **3**

S2 Stationary spectroscopy **4**

S3 Time-correlated single photon counting **5**

S4 Femtosecond fluorescence up-conversion **6**

S5 Electronic transient absorption spectroscopy (TA) **7**

S6 Molecular dynamics simulations and quantum-chemical calculations **10**

List of Figures

S1 Electron donors tested in this study. 3
S2 CD and absorption spectra measured with **1** and **2** in water (top), and stationary absorption and emission spectra of **1** in different solvents (bottom). 4
S3 TCSPC fluorescence decays measured with **1** in various solvents and best-fits of the convolution of the instrument response function (grey) with a single exponential function. 5
S4 Pure quenching dynamics of the fluorescence of the two enantiomers of **1** with 0.15 M of either BINOL enantiomer in DCM. 6
S5 Pure quenching dynamics of the fluorescence of the two enantiomers of **1** with 0.15 M of either BINOL enantiomer in THF. 6
S6 Comparison of the evolution-associated difference spectra (EADS) obtained from the global analysis of the transient-absorption data measured with (–)-**1** with 50 mM of either D-Trp or L-Trp in 60:40 (v/v) water/ethanol (top) and 90:10 (v/v) water/ACN (bottom). Because of the larger IRF at shorter wavelength, the shape of EADS A below 420 nm should be considered with caution. 7
S7 A) Comparison of the evolution-associated difference spectra obtained from the global analysis of the transient-absorption data measured with (+)-**1** with 50 mM of either (+)- or (–)-BINOL in ACN. An early transient absorption spectrum recorded with (+)-**1** alone is also shown. B) Time evolution of the transient absorption at 360 nm (dashed line in panel A). 8
S8 A) Comparison of the evolution-associated difference spectra obtained from the global analysis of the transient-absorption data measured with (+)-**1** with 0.15 M of either (+)- or (–)-BINOL in DCM. 9
S9 Histograms of the centre-of-mass AD distance (A) and radial-distribution functions (B) obtained from 50 ns MD trajectories of (–)-**1** and Trp in water. 11
S10 Frontier molecular orbitals of **1**, Trp and BINOL calculated at the DFT level (B3LYP/6-31G+d). 12
S11 Histograms of the minimum AD distance obtained from 50 ns MD trajectories of (–)-**1** and one BINOL molecule in acetonitrile. 13
S12 Radial-distribution functions obtained from 50 ns MD trajectories of (–)-**1** and 11 BINOL molecules in acetonitrile. 14
S13 Histograms of the centre-of-mass AD distance obtained from 50 ns MD trajectories of (–)-**1** and one BINOL molecule in THF. 14
S14 Histograms of the minimum (A) and centre-of-mass distance (B) between (–)-**1** and BF_4^- obtained from 50 ns MD trajectories in acetonitrile and THF. 15

List of Tables

S1 Driving force for photoinduced electron transfer, $-\Delta G_{ET}$, between the cationic [6]helicenes **1** and **2** and the electron donors in polar solvent estimated from the Weller equation with the redox potentials of the reactants. 3

S1 Samples

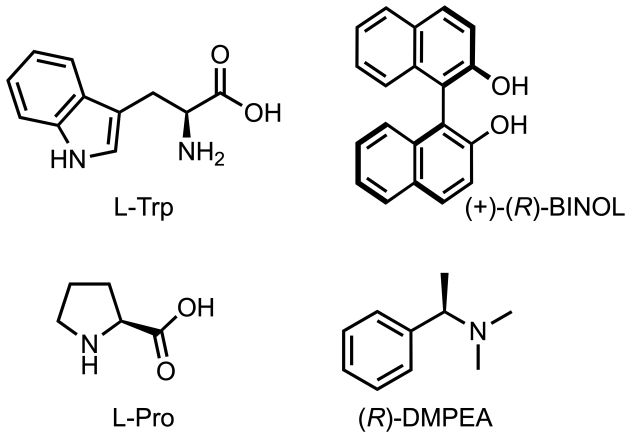

Figure S1: Electron donors tested in this study.

Table S1: Driving force for photoinduced electron transfer, $-\Delta G_{ET}$, between the cationic [6]helicenes **1** and **2** and the electron donors in polar solvent estimated from the Weller equation with the redox potentials of the reactants.

A/D	$-\Delta G_{\mathrm{ET}}$ / eV	E_{red}(A)/ V. vs. SCE	E_{ox}(D)/ V. vs. SCE
1/TrP	0.86	-0.52[a]	0.77[b]
2/TrP	0.49	-0.85[a]	0.77[b]
1/BINOL	0.73	-0.52	0.90[c]
1/Pro	0.22	-0.52	1.41[d]
2/Pro	-0.10	-0.85	1.41
1/DMPEA	0.89	-0.52	0.74[e]
2/DMPEA	0.36	-0.52	0.74

[a] from ref.1; [b] from ref.2;[c] value for naphthol from ref.3; [d] from ref.4; [e] from ref.5.

S2 Stationary spectroscopy

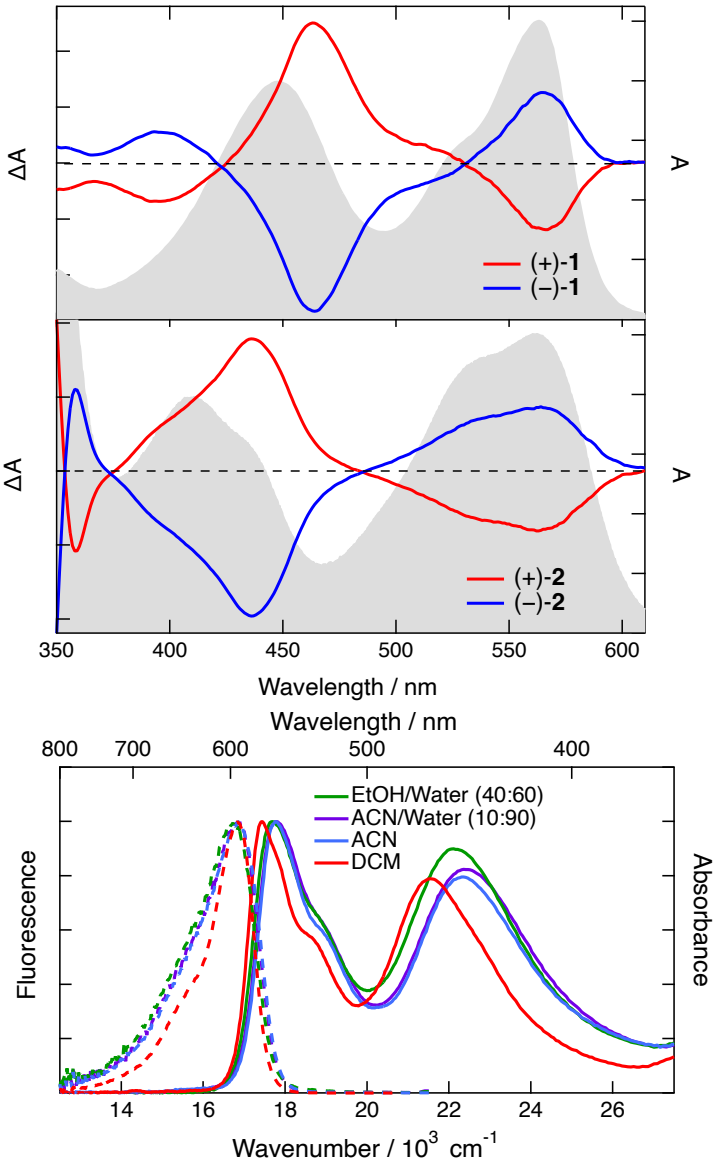

Figure S2: CD and absorption spectra measured with **1** and **2** in water (top), and stationary absorption and emission spectra of **1** in different solvents (bottom).

S3 Time-correlated single photon counting

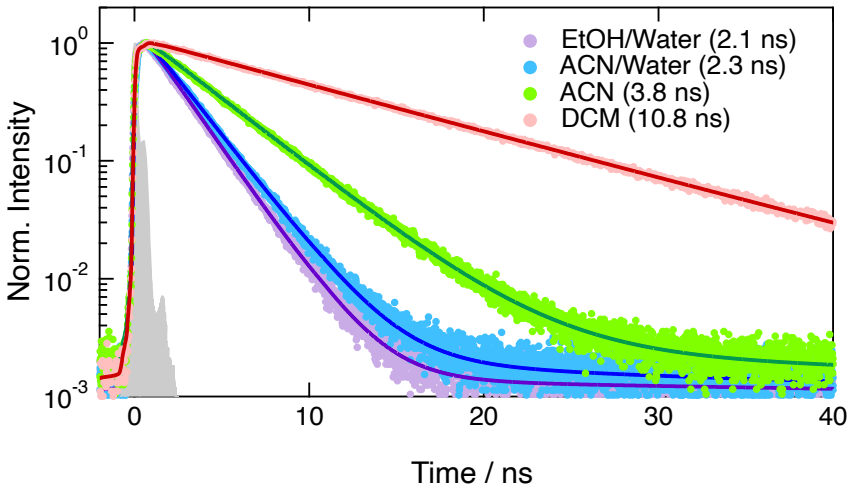

Figure S3: TCSPC fluorescence decays measured with **1** in various solvents and best-fits of the convolution of the instrument response function (grey) with a single exponential function.

S4 Femtosecond fluorescence up-conversion

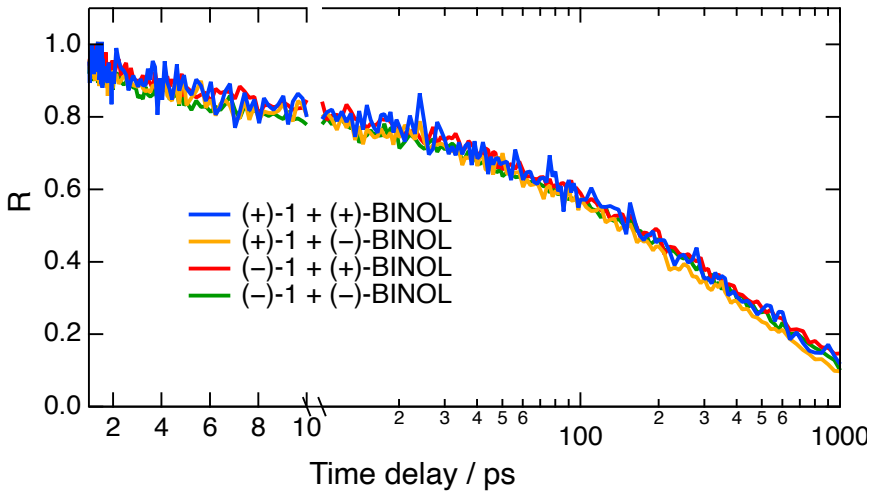

Figure S4: Pure quenching dynamics of the fluorescence of the two enantiomers of **1** with 0.15 M of either BINOL enantiomer in DCM.

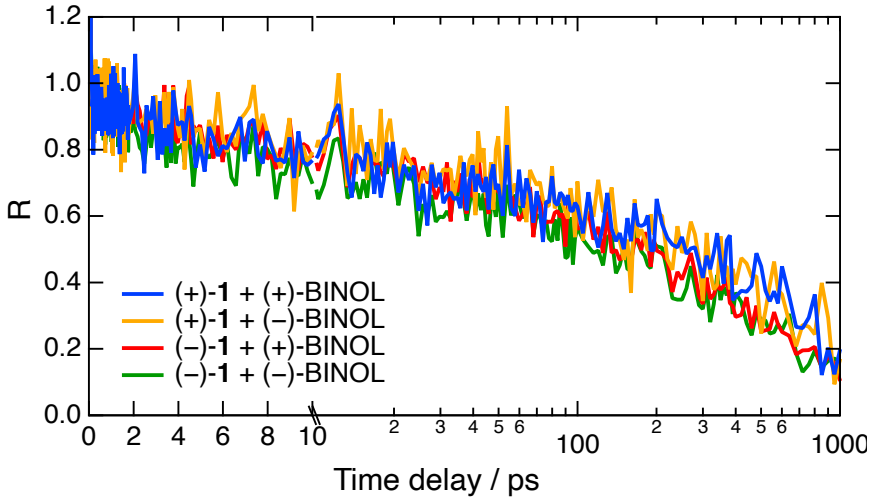

Figure S5: Pure quenching dynamics of the fluorescence of the two enantiomers of **1** with 0.15 M of either BINOL enantiomer in THF.

S5 Electronic transient absorption spectroscopy (TA)

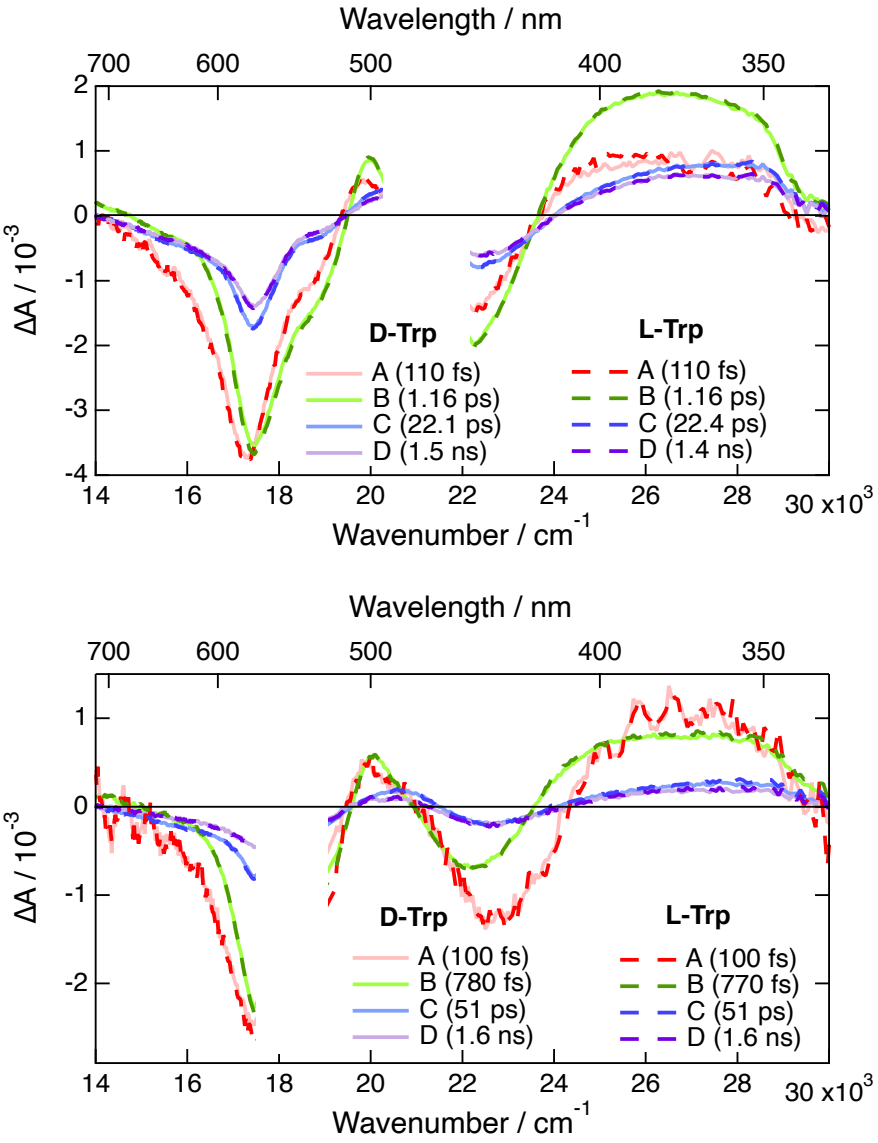

Figure S6: Comparison of the evolution-associated difference spectra (EADS) obtained from the global analysis of the transient-absorption data measured with (–)-**1** with 50 mM of either D-Trp or L-Trp in 60:40 (v/v) water/ethanol (top) and 90:10 (v/v) water/ACN (bottom). Because of the larger IRF at shorter wavelength, the shape of EADS A below 420 nm should be considered with caution.

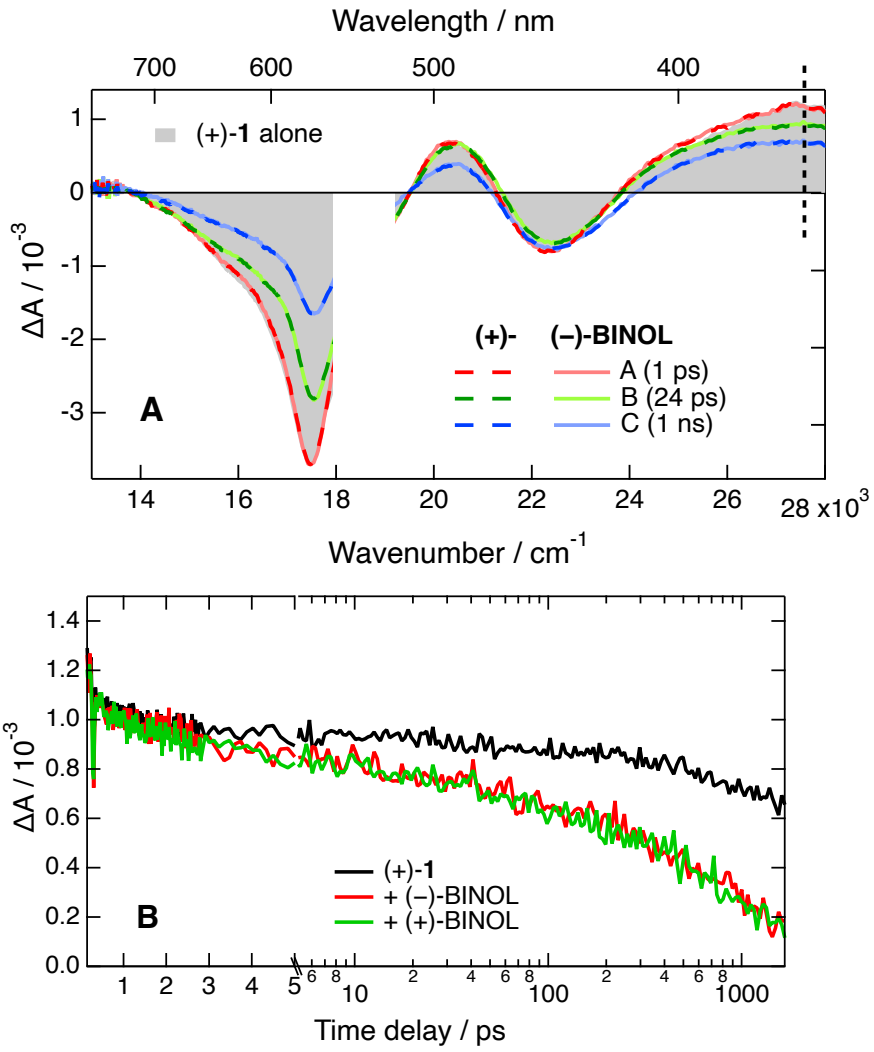

Figure S7: A) Comparison of the evolution-associated difference spectra obtained from the global analysis of the transient-absorption data measured with (+)-**1** with 50 mM of either (+)- or (–)-BINOL in ACN. An early transient absorption spectrum recorded with (+)-**1** alone is also shown. B) Time evolution of the transient absorption at 360 nm (dashed line in panel A).

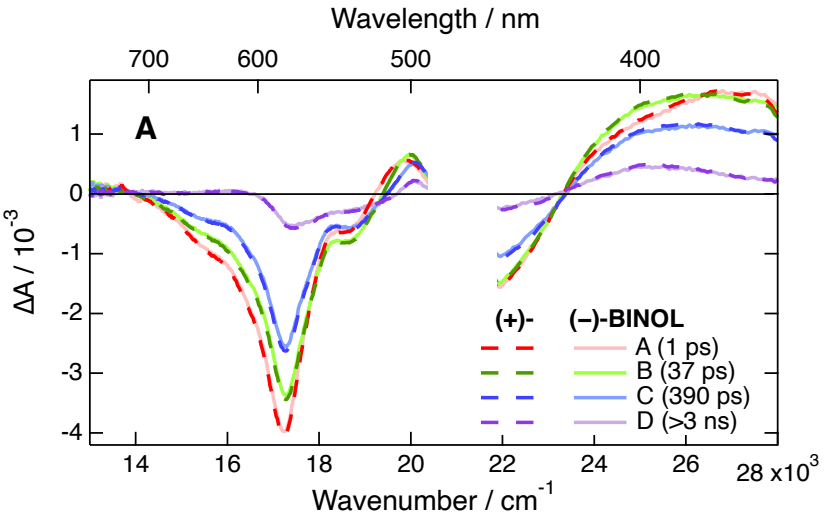

Figure S8: A) Comparison of the evolution-associated difference spectra obtained from the global analysis of the transient-absorption data measured with (+)-**1** with 0.15 M of either (+)- or (–)-BINOL in DCM.

S6 Molecular dynamics simulations and quantum-chemical calculations

The potential for the dihedral angle of BINOL was described as:

$$V_d(\phi) = k_\phi(1 + \cos(n\phi - \phi_s)). \tag{S1}$$

The parameters were determined by fitting eq.S1 to the potential obtained from relaxed-scan calculations of the energy of BINOL as a function of the dihedral angle, ϕ. The best-fit parameters were: $k_\phi = 35.89\,\mathrm{kJ/mol}$; ϕ_s=88.3 deg. and $n = 1$. The force-field parameters for BF_4^- were taken from ref.6.

Non-bonded interactions were evaluated with a cutoff of 1.4 nm, and long-range electrostatic interactions were accounted for by the particle mesh Ewald method,[7] with 0.12 nm grid spacing and forth-order interpolation. A long-range dispersion correction for energy was also included. The LINCS algorithm[8] was used to constrain the bonds of all system components with the exception of water, for which the SETTLE algorithm was applied.[9] The equilibration of the system was ensured by inspecting the total energy drift. The isothermal-isobaric ensemble, NPT, was used for all productions with the v-rescale thermostat at 295 K,[10] and the Parrinello-Rahman barostat at 1 atm using coupling constants of 0.5 ps and 3 ps respectively.[11]

For the simulations of **1** and one Trp, the 5x5x5 nm^3 box was filled with 4209 water molecules. For the simulations of **1** and 11 BINOL, the box was filled with 1420 molecules of acetonitrile. For the simulations with one BINOL, either 1440 acetonitrile or 924 THF molecules were added.

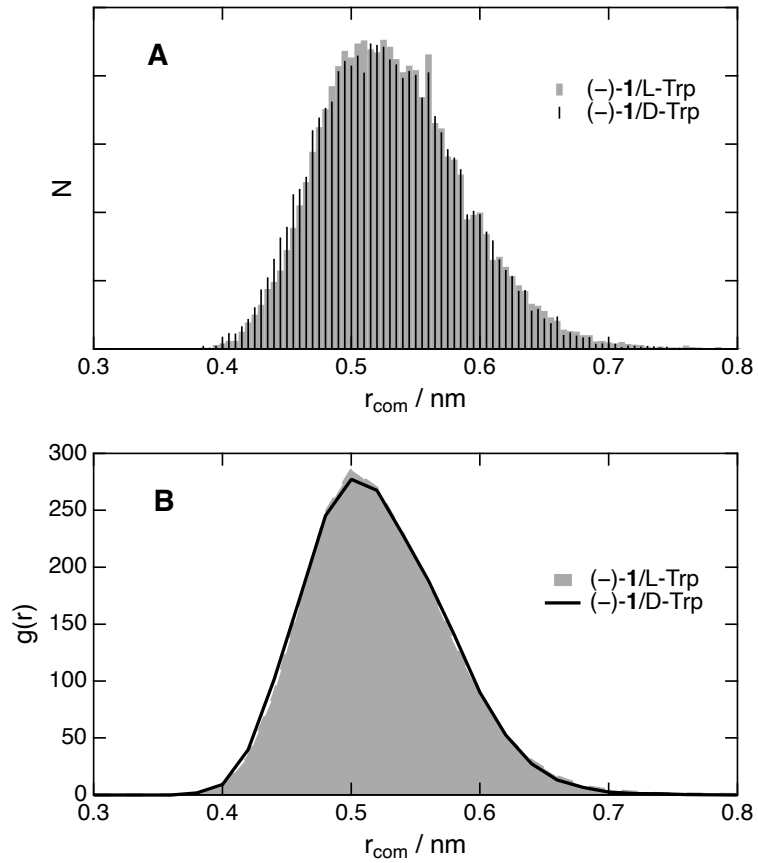

Figure S9: Histograms of the centre-of-mass AD distance (A) and radial-distribution functions (B) obtained from 50 ns MD trajectories of (–)-**1** and Trp in water.

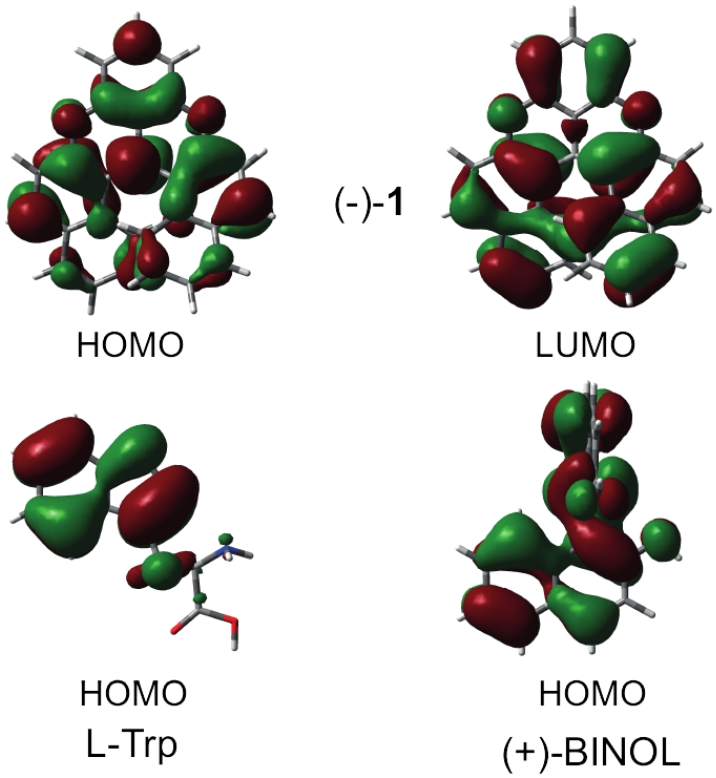

Figure S10: Frontier molecular orbitals of **1**, Trp and BINOL calculated at the DFT level (B3LYP/6-31G+d).

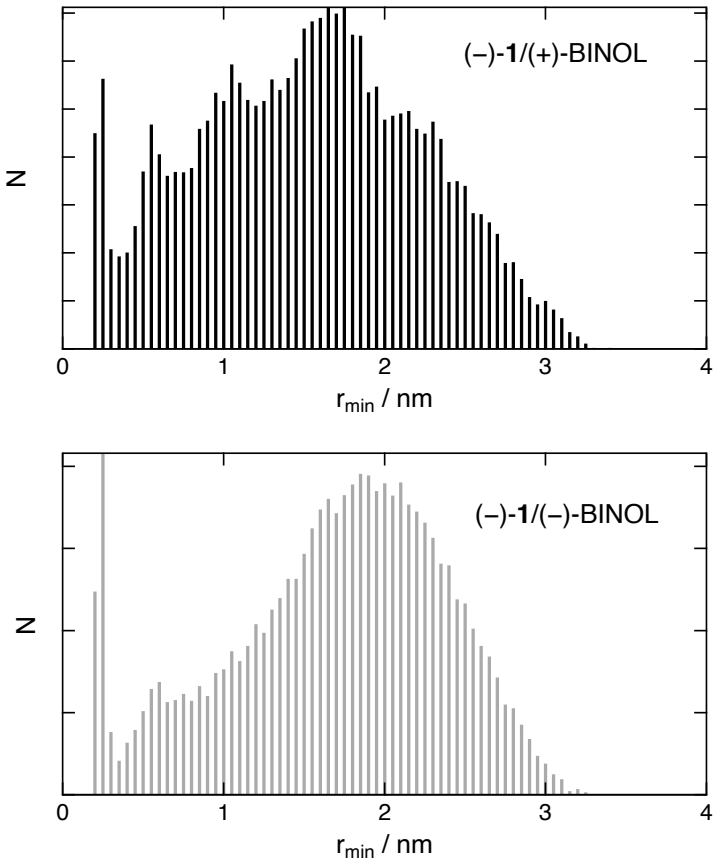

Figure S11: Histograms of the minimum AD distance obtained from 50 ns MD trajectories of (–)-**1** and one BINOL molecule in acetonitrile.

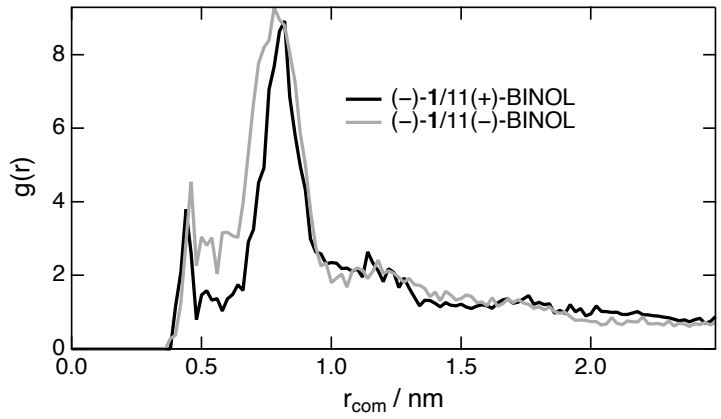

Figure S12: Radial-distribution functions obtained from 50 ns MD trajectories of (–)-**1** and 11 BINOL molecules in acetonitrile.

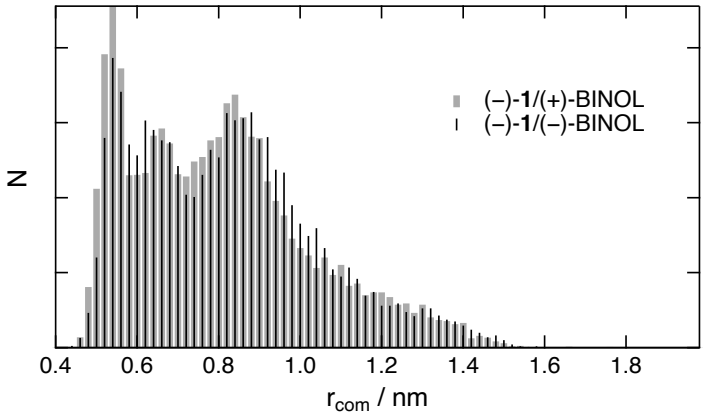

Figure S13: Histograms of the centre-of-mass AD distance obtained from 50 ns MD trajectories of (–)-**1** and one BINOL molecule in THF.

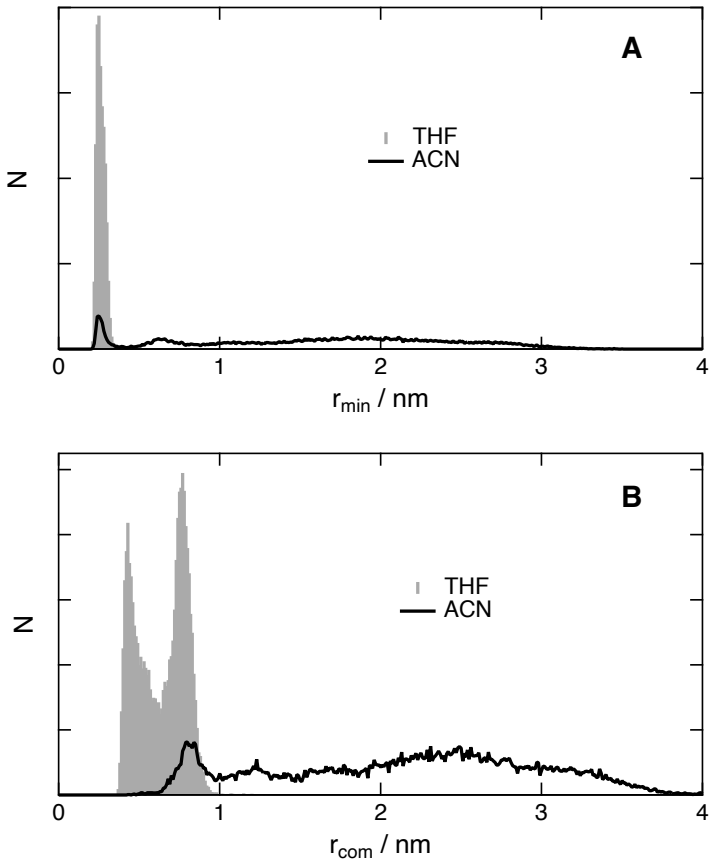

Figure S14: Histograms of the minimum (A) and centre-of-mass distance (B) between (–)-**1** and BF_4^- obtained from 50 ns MD trajectories in acetonitrile and THF.

References

[1] J. Bosson, G. M. Labrador, S. Pascal, F.-A. Miannay, O. Yushchenko, H. Li, L. Bouffier, N. Sojic, R. C. Tovar, G. Muller, D. Jacquemin, A. D. Laurent, B. Le Guennic, E. Vauthey and J. Lacour, *Chem. Eur. J.*, 2016, **22**, 18394–18403.

[2] A. Harriman, *J. Phys. Chem.*, 1987, **91**, 6102–6104.

[3] R. E. Sioda and B. Frankowska, *J. Electroanal. Chem.*, 2004, **568**, 365–370.

[4] T. Shoji, S. Kim, K. Yamamoto, T. Kawai, Y. Okada and K. Chiba, *Org. Lett.*, 2014, **16**, 6404–6407.

[5] L. Meites, *Electrochemical Data. Part 1: Organic, Organometallic, and Biochemical Substances*, J. Wiley, 1974.

[6] B. Doherty, X. Zhong, S. Gathiaka, B. Li and O. Acevedo, *J. Chem. Theory Comput.*, 2017, **13**, 6131–6145.

[7] T. Darden, D. York and L. Pedersen, *J. Chem. Phys.*, 1993, **98**, 10089–10092.

[8] B. Hess, H. Bekker, H. J. C. Berendsen and J. G. E. M. Fraaije, *J. Comput. Chem.*, 1997, **18**, 1463–1472.

[9] S. Miyamoto and P. A. Kollman, *Proteins: Struct., Funct., Genet.*, 1993, **16**, 226–245.

[10] G. Bussi, T. Zykova-Timan and M. Parrinello, *J. Chem. Phys.*, 2009, **130**, 074101.

[11] M. Parrinello and A. Rahman, *J. Appl. Phys.*, 1981, **52**, 7182–7190.